Isotope effects in liquid water probed by x-ray Raman spectroscopy

U. Bergmann,[1] D. Nordlund,[1] Ph. Wernet,[1,2] M. Odelius,[3] L. G. M. Pettersson,[3] and A. Nilsson[1,3]
[1]*Stanford Synchrotron Radiation Laboratory, P.O. Box 20450, Stanford, California 94309, USA*
[2]*BESSY, Albert-Einstein-Strasse 15, D-12489 Berlin, Germany*
[3]*FYSIKUM, Stockholm University, AlbaNova, S-106 91 Stockholm, Sweden*
(Received 1 May 2007; published 5 July 2007)

The isotope effect on the local structure of liquid water at room temperature is studied by x-ray Raman spectroscopy. The difference between the room-temperature spectra of liquid H_2O and D_2O is compared to the difference spectrum between liquid H_2O at 22 and 2 °C. The spectral changes between H_2O and D_2O can partly be attributed to structural changes similar to a temperature change, in agreement with diffraction data. Additionally, we find that isotope substitution affects the local asymmetry in the hydrogen-bonded network: hydrogen-bonding configurations are more asymmetric on the donor side for H_2O than for D_2O. A cluster model is used to computationally illustrate the spectral changes that arise due to the increased asymmetry, capturing all essential features in the difference spectrum. We infer from our study that quantum effects contribute to the formation of asymmetrical species in the liquid.

DOI: 10.1103/PhysRevB.76.024202 PACS number(s): 61.20.−p, 61.10.Ht, 61.25.Em, 78.70.Dm

The structure of liquid water is one of the most important scientific topics with an enormous impact on nearly all processes in chemistry and biology. In recent years, a debate on water structure has emerged from x-ray absorption (XA) studies using x-ray Raman scattering (XRS) and conventional x-ray absorption spectroscopy (XAS), reporting that liquid water has a large fraction of asymmetrically hydrogen-bonded species, with one strong and one weak donor hydrogen bond (H bond).[1] This is in sharp contrast to the widely held picture of symmetrically H-bonded species upon melting the tetrahedral structure in ice, as indicated by interpretations of x-ray and neutron-diffraction data and as also deduced from molecular-dynamics (MD) simulations. The interpretation of the diffraction data in terms of structural models is not straightforward, however.[2,3] Although x-ray diffraction provides the Fourier transform of the electron density, mainly corresponding to the O-O radial distribution function, the limited Q range available has precluded simple inversion of the data. The analysis has instead been performed either through comparison with structures from MD simulation models[4] or by modifying an initial model interaction potential.[5] It has only recently been realized that in both cases a bias toward symmetric solutions is built into the analysis;[2,3] the diffraction data are, in fact, surprisingly insensitive and allow a range of solutions, although the specific, both symmetric and asymmetric, solutions in Refs. 2 and 3 have been criticized on various grounds.[3,6] The situation is thus somewhat unclear and there is at present an intense debate regarding the interpretation and impact of the XA results.[2,3,7–11] This is due to the challenge to the textbook picture of liquid water and the fact that current MD simulations do not reproduce the large number of asymmetrical species required for agreement with the interpretation of the XA data.[1] To underline the discrepancy, it was recently shown that an even stricter asymmetry criterion is necessary to obtain the correct line shape of the XA data and it is naturally of great interest to determine what underlying effects could generate the proposed asymmetry.[10] In the present contribution, we use liquid H_2O and D_2O to show that quantum effects may contribute to the observed asymmetry.

Light and heavy liquid water, H_2O and D_2O, differ in numerous macroscopic properties such as boiling point, viscosity, and heat capacity.[12] The differences upon H/D substitution in thermodynamical properties, intra- and intermolecular dynamical behavior, and associated structural changes are usually denoted isotope quantum effects. In early γ-ray and hard x-ray experiments, differences upon H/D substitution in the O-O partial radial distribution functions of liquid water were observed.[13] As proposed by Root *et al.*[14] in 1986 and further elaborated by, e.g., Wilse Robinson and co-workers,[15] H_2O at room temperature is similar to D_2O if the temperature of the latter is raised by ~5 °C and the density increased by ~0.5%. Recent x-ray-diffraction studies[16] have corroborated this observation. Investigating the H_2O-D_2O difference is an experimental way of addressing the so-called quantum effects in liquid water as studied in numerous theoretical investigations. Using path-integral techniques, different degrees of freedom can be quantized in Car-Parrinello MD or Monte Carlo simulations.[17] Comparison with the classical case from these studies shows improved agreement with, e.g., x-ray-diffraction data when these effects are included. The broadened O-H peak from inclusion of quantum effects and the larger width over that of the O-D correlation have been taken by Hernández de la Peña and Kusalik[18] as indicative of a possibly higher tunneling frequency in the librational motion for H_2O over D_2O. This was suggested as a possible explanation of the isotope effect, but direct experimental measurement of the H-bond switching in gas phase for cyclical water pentamers shows a much too low frequency to render this plausible[19] although in excited states of librational motion the frequency could be significantly higher.[20] A rather different approach is the quantum cluster equilibrium theory,[21] which qualitatively supports the XA data.[9] When applied to isotope substitution in water,[22] structural changes different from zero-point-induced thermal offset effects are seen in the population of different clusters.

We have used XRS to probe the difference between liquid H_2O and D_2O at room temperature (RT) and compare with

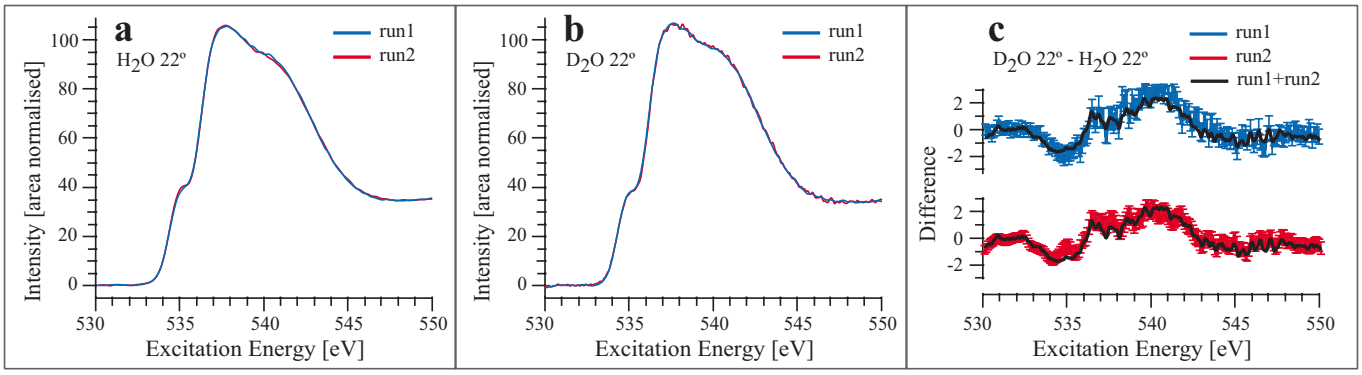

FIG. 1. (Color online) XRS spectra recorded from two independent experimental runs, (a) H_2O at 22 °C and (b) D_2O at 22 °C, and (c) the isotope difference spectra, H_2O-D_2O at 22 °C. Also, the isotope difference spectrum from the averaged spectra (run 1+run 2) is plotted for comparison. The error bars in the difference spectra, based on the Poisson distribution of total counts from the detector, are plotted with a confidence interval of 68%. Spectra from run 1 and run 2 are nearly identical, and the isotope difference spectra from the two runs are very well reproduced (Ref. 28).

the differences observed when cooling RT H_2O. The high accuracy and stability of XRS (see also Refs. 8 and 11) are essential to acquire the small spectral changes generated by isotope substitution. As applied here with low momentum transfer, XRS probes excitations of oxygen (O) 1*s* electrons to the valence unoccupied molecular orbitals of water with *p* character analogous to XAS.[8,23] H bonding affects the electronic structure of water and structural changes in the liquid associated with changes in the local H-bonding environment can thus effectively be probed with XRS.[24,25]

The experiments were performed at the undulator beamline 18-ID at the Advanced Photon Source, equipped with a Si (111) double crystal monochromator. Raman scattering was analyzed with a new high-energy-resolution multicrystal spectrometer in a vertical Rowland geometry using a cluster of seven Si (440) analyzer crystals (100 mm diameter, 1 m radius) at a fixed Bragg angle of 88°. This setup selects 6.46 keV photons with a resolution of ~0.3 eV. The analyzer cluster was set to a Raman scattering angle of 45±9 ° in the horizontal plane, corresponding to momentum transfers of $q=2.6\pm0.5$ Å^{-1}, which is well within the dipole limit for water O 1*s* scattering (see supplementary material of Ref. 1). The monochromator energy was scanned from 6990 to 7060 eV with a flux of $\sim10^{13}$ photons/s focused down to a 0.1×1 mm^2 spot size. The overall energy resolution amounted to ~1 eV full width at half maximum (FWHM). A photon counting Si drift detector was used for data collection. Spurious scattering signal from oxygen in air was avoided by having the x-ray paths to and from the samples in a He environment. Because the spectral changes between H_2O and D_2O are very small, the measurements were repeated in a later, independent experimental run to ensure reproducibility of the observed changes. A potential concern is radiation damage. Note that the interaction time of x rays with the water molecule in absorption, as well as in XRS, is so short that any damage to the probed molecule does not affect the absorption spectrum.[26] Therefore, any possible spectral distortion can only result from a second interaction with an already damaged molecule. In the case of a liquid at our incident flux density, this is very unlikely because of (a) the high mobility of the water molecules and (b) the extremely low XRS cross section. The issue of radiation damage has been addressed in the present work and in several of the previous experiments.[1,24] We consistently find that there is no difference between spectra taken with flowing water [flowing speed of ~1 m/s (8 l/min)] and spectra taken with stationary water when contained in a reservoir of sufficient size (we used an ~100 ml beaker).[27]

We used de-ionized water (~18 MΩ cm) for the H_2O measurements and D_2O as purchased from Sigma Aldrich (D atom purity is 99.9%). The hygroscopic D_2O was kept isolated from air by a lid, and all spectra were recorded under atmospheric pressure. In both runs, spectra were obtained by averaging multiple sweeps. The observed XRS signal was typically 700 counts/s (at 537 eV energy transfer) with a Compton background of ~100 counts/s (at 530 eV). The averaged spectra had total counts of 40 000 for H_2O (50 000 for D_2O) in run 1 and 60 000 for H_2O (20 000 for D_2O) in run 2 at 537 eV. The spectra were normalized to the incident photon flux measured with a gas-filled ion chamber, and the background, mainly from Compton scattering, was subtracted. Various background functions were tested. We found that over the small energy range of the near edge region, no significant differences between linear and higher-order polynomial background functions were observed. Thus, we chose to subtract a linear background. The energy axis was calibrated by aligning the energy transfer of H_2O with soft x-ray H_2O absorption spectra.[24]

In run 1, liquid H_2O flowed through a sample cell with a 1 μm-thick Si_3N_4 window using a temperature-controlled circulating bath. *K*-type thermocouples were used to measure the water temperature. In the second run, H_2O was stationary in a plastic beaker with a 1 μm Si_3N_4 window. In both runs, D_2O was kept stationary in a sample beaker. In run 1, we used a 25 μm-thick Kapton window, and in run 2 we used a 1 μm-thick Si_3N_4 window. When using the Kapton window, a small spectral contribution from the oxygen in the Kapton was observed. It was subtracted using a measured Kapton *K*-edge spectrum. Figure 1 shows the comparison of RT spectra from both runs for (a) H_2O and (b) D_2O as well as (c) the difference spectrum D_2O-H_2O.[28] This comparison demonstrates that even under slightly different experimental con-

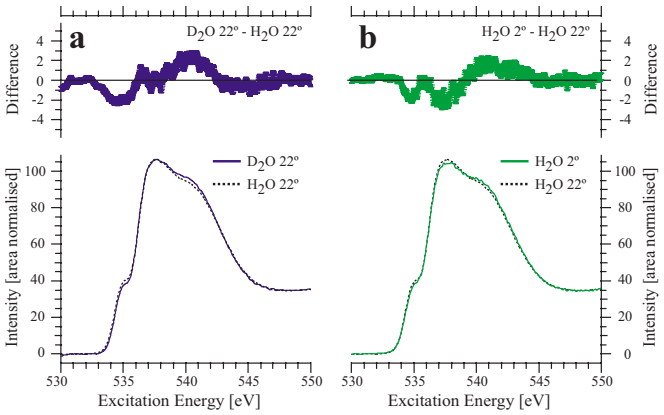

FIG. 2. (Color online) XRS spectra of liquid D_2O at 22 °C [(a), solid line] and liquid H_2O at 2 °C [(b), solid line] compared to H_2O at 22 °C [(a) and (b), dashed line]. Top panels: Difference of the spectra in the bottom panels [(a) D_2O-H_2O at 22 °C, (b) H_2O 2 °C−H_2O 22 °C]. The error bars in the difference spectra, based on the Poisson distribution of total counts from the detector, are plotted with a confidence interval of 68% (Ref. 28).

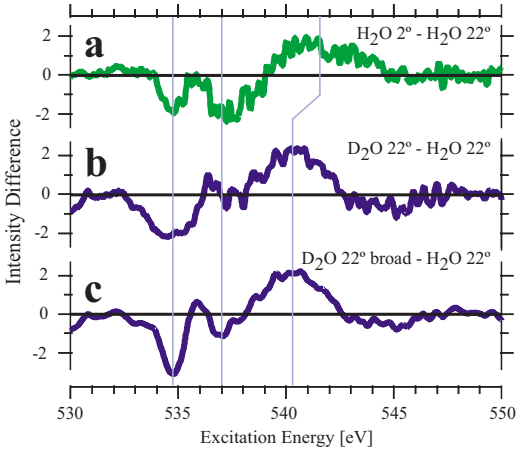

FIG. 3. (Color online) O *K*-edge XRS isotope and temperature difference spectra. The spectra are plotted without the error bars shown in Fig. 1. Vertical lines (gray) are drawn as a guide for the eyes for the preedge, the main edge, and the postedge. From top to bottom: (a) H_2O 2 °C−H_2O 22 °C, (b) D_2O-H_2O at 22 °C, and (c) the D_2O-H_2O difference at 22 °C taken after a Gaussian broadening with full width at half maximum of 0.5 eV of the D_2O spectrum (Ref. 28).

ditions (i.e. flow versus stationary and Kapton versus Si_3N_4 window), the spectra are nearly identical. In particular, the shape of the difference spectra is very well reproduced. We therefore averaged the H_2O and D_2O spectra from the two runs, respectively, and the subsequent analysis and discussion is based on these averaged spectra.

Figure 2 shows the O *K*-edge XRS spectra of (a) liquid D_2O at RT and (b) liquid H_2O at low temperature. Both spectra are compared to the RT H_2O spectrum used as a reference in the following (dashed). In the top panel, the respective difference spectra are plotted with statistical error bars. We note that there are similarities between the differences upon H/D substitution and the changes induced by decreasing the temperature of H_2O water. However, small but significant dissimilarities are discernible between the two difference spectra.

We discuss the liquid water spectrum in terms of three energy regions: 534–536 eV (preedge region), 536–538.8 eV (main-edge region), and 538.8–545 eV (postedge region).[1] Both when melting ice into liquid water and when heating the liquid, intensity in the preedge and main-edge regions increases, whereas intensity in the postedge region decreases.[1] The experimental spectra have been suggested to indicate a large fraction (more than 60%) of strongly asymmetrical species.[1,10] Such single-donor (SD) species have one of the H bonds on the donor side significantly weakened, in sharp contrast to more symmetrically H-bonded tetrahedral-like double-donor (DD) species. Increasing the temperature increases the fraction of SD species at the cost of DD species. The temperature difference spectrum in Fig. 1(b) shows all salient features of this interconversion of species, differing only by a multiplicative factor from previously published difference spectra for various temperature changes.[1,8] Due to the similar intensities of the difference spectra in Figs. 1(a) and 1(b), we can infer that part of the isotope effect in Fig. 1(a) is similar to a temperature change of 20 °C or less. This indicates a slightly larger population of asymmetric SD species in H_2O as compared to D_2O. However, as indicated above, the isotope difference spectrum [Fig. 1(a)] is not simply related by a multiplicative factor to the temperature difference spectrum [Fig. 1(b)] which indicates an additional structural effect upon isotope substitution. How can we understand this additional effect in terms of spectral features?

In Fig. 3, we compare in more detail (b) the D_2O-H_2O difference spectrum with (a) the H_2O 22 °C−2 °C difference spectrum. Vertical lines are drawn as a guide for the eyes of the three spectral regions described above (pre-, main-, and postedge regions). Compared to the temperature difference spectrum, several dissimilarities are observed in the isotope difference spectrum: (1) the preedge feature is broader, (2) the decrease in preedge intensity is larger, (3) the main-edge region decreases less (if at all), (4) the postedge feature is symmetric and shifted to lower energies (lacking the higher-energy component around 543 eV seen in the temperature difference spectrum), and (5) around 543–546 eV a decrease is discernible.

The preedge in liquid water is due to an internal O-H antibonding state which is localized on the weakly bonded donor side in SD species,[29] and it has Franck-Condon broadening due to the zero-point distribution of H (D) in the molecule. A more confined distribution of D in space is expected to produce a narrower distribution of excitation energies,[30] i.e., a sharper preedge peak. By displaying differences, we can see the narrowing of the preedge peak in D_2O even at our experimental energy resolution of 1 eV. For comparison with H_2O, this narrowing effect can be compensated by convoluting the D_2O spectrum with a Gaussian function, which in this case was chosen to have 0.5 eV FWHM. Comparison of the difference spectrum using the thus broadened D_2O spectrum [Fig. 3(c)] with the spectrum in Fig. 3(b) shows that the effect of the broadening in the difference spectrum is limited to the shape of the preedge region. The width of the

preedge peak in Fig. 3(c) is now comparable to the width in Fig. 3(a) but significant dissimilarities remain. What is the structural change that causes the preedge to decrease without a decreasing main edge and that causes the postedge feature to shift to lower energies?

SD species are associated with the preedge intensity and, as seen in the temperature difference data [Fig. 2(a) and Refs. 1, 8, and 10], also contribute more than the DD species to the main-edge intensity. The relative strength of the preedge intensity in H_2O can be understood as follows. The weaker the weak donor bond becomes, the more the associated preedge state localizes and gains p character, giving higher dipole transition amplitude in the XA process.[1,29] A higher preedge peak intensity can therefore be associated with a further weakening of the weak donor bond in SD species, either by elongation or bending.[1] As manifested in the difference spectra (see Fig. 3) through the increase in preedge intensity and the shift in postedge position (see below), liquid H_2O thus has SD species with larger asymmetry on the donor side than do SD species in D_2O.

The observable energy shift of the postedge is related to changes in the local H-bond length according to the established concept of "bond length with the ruler."[10,26] In the XA spectrum of liquid water and ice, the postedge resonance is attributed to excitations into antibonding states mostly located along the donating H bond.[1,29] Since these states are antibonding not only in terms of the intramolecular OH σ bond but also with respect to the intermolecular donating H bond, the energy position of the postedge becomes sensitive to the H-bond distance. In particular, a shorter H-bond distance increases the energy of the intermolecular antibonding states and consequently the energy of the postedge resonance in the absorption spectrum.[10] For water, this is demonstrated experimentally in, e.g., protonated water where the short H-bond length ($\sim$2.5 Å) in the eigenform (H_3O^+) causes an upward shift in the postedge resonance of 1 eV at high proton concentration.[31] Based on the changes in the difference spectra shown in Fig. 2 and on comparison to protonated water,[10] H_2O appears to have species where the strong donating H bonds are shorter as compared to D_2O. What is the likely origin of the H-bond shortening in H_2O?

In ice, consisting exclusively of DD species, there is no significant difference between the H-bond length in H_2O versus D_2O ice (less than 0.01 Å, see, e.g., Ref. 32), which suggests that the deduced bond-length changes in the liquid are associated with the SD and not with the DD species. It is interesting to note that calculations on small clusters suggest that, due to the asymmetry in H bonding, the intact H bonds in SD configurations are shorter (stronger)[33] as compared to the H bonds in DD configurations.

Our experimental finding holds that the isotope effect, in addition to a temperature offset (i.e., change of populations as a result of H-bond breakage and/or weakening[1,8]), can be attributed to an increase of asymmetry mainly of SD species in H_2O with some possible minor contributions from DD species. This is further investigated in Fig. 4, where cluster models of both asymmetric and symmetric species are used to simulate the spectral changes associated with local changes in the H-bond network; the spectra were calculated using the StoBe-deMon code[34] as in Ref. 10. This all-

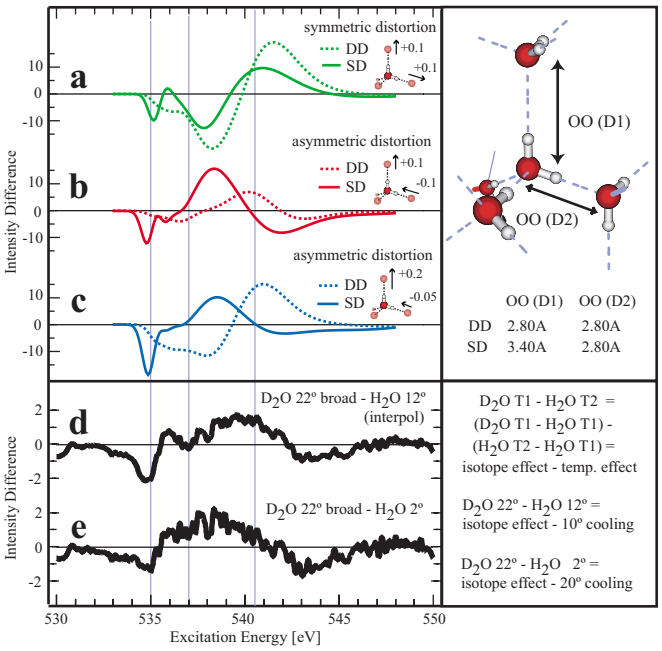

FIG. 4. (Color online) Comparison of model calculations with measured spectra. (Top) Calculated spectra illustrate the effect of changes to the H-bond lengths starting from two different geometries: an icelike (DD) cluster (dotted lines) with O-O distances of 2.80 Å and an asymmetric (SD) cluster (solid lines) generated by increasing the H-bond distance of one of the donors by 0.6 Å (O-O D1). Difference spectra of the distorted minus original cluster are shown for (a) elongation of both donating H bonds by 0.1 Å and (b) elongation of the weak donor H bond (O-O D1) by 0.1 Å and shortening of the strong donor H bond (O-O D2) by 0.1 Å (for DD species, the original D1 and D2 bonds are equivalent). (c) Similar to (b) but with a 0.2 Å elongation and 0.05 Å shortening. (Bottom) Experimental difference spectra of (d) D_2O at 22 °C minus H_2O at 12 °C (linearly interpolated from the spectra at 2 and 22 °C) and (e) D_2O at 22 °C minus H_2O at 2 °C, representing the isotope effect with a temperature effect subtracted (Ref. 28).

electron, density-functional theory based technique has been successfully applied to, e.g., the analysis of bulk spectra of methanol[35] as well as the structural changes due to protonated water.[31] Here, we start from an icelike (DD) cluster (with O-O distances of 2.80 Å) and generate a typical SD species by increasing the H-bond distance of one of the donor bonds by 0.6 Å (O-O D1 in the figure). The simulated cluster consists of 42 molecules and includes water molecules up to three H bonds from the central core-excited oxygen, but only the central pentamer is shown in Fig. 4. Difference spectra of clusters in the original and in various distorted geometries are shown in Figs. 4(a)–4(c), where the absolute intensity difference is obtained by using the same area normalization as for the experimental spectra.[28] We investigate the effect of structural changes in the SD and the DD motifs: symmetrically [Fig. 4(a)] by increasing both donor bonds by 0.1 Å and asymmetrically [Fig. 4(b)] by elongating the weak donor H bond (O-O D1) by 0.1 Å, and shortening the strong donor H bond (O-O D2) by 0.1 Å (for DD species, the original D1 and D2 bonds are equivalent). The asymmetric distortion in Fig. 4(c) has more elongation

(0.2 Å) and less shortening (0.05 Å) compared to that in Fig. 4(b). These simulated spectral changes are compared to experimental isotope difference spectra where temperature effects of 10 °C [Fig. 4(d)] and 20 °C [Fig. 4(e)] have been subtracted (Fig. 4(d), e.g., $D_2O(22\ °C) - H_2O(12\ °C) = [D_2O(22\ °C) - H_2O(22\ °C)] - [H_2O(22\ °C) - H_2O(12\ °C)]$).

We note that symmetric expansions [Fig. 4(a)] lead to results that are qualitatively different from all measured difference spectra. They show very poor agreement in the postedge and higher regions for both SD and DD starting structures. For symmetric contraction (not shown), the difference spectra are close to the inverse of the symmetric expansion, with poor agreement in the preedge and main-edge regions. On the other hand, for an enhanced asymmetry of the SD species [Figs. 4(b) and 4(c)], this simple model reproduces the salient features of the experimental differences [Figs. 4(d) and 4(e)]. The preedge decreases (for D_2O) and the postedge shifts to lower (higher) energy for D_2O (H_2O), and above 543 eV the loss of intensity for D_2O is reproduced. Further elongation and less shortening [Fig. 4(c)] improves the agreement with the spectrum shown in Fig. 4(d) as the preedge decrease becomes more pronounced and the postedge shift less dramatic. For asymmetric distortions around DD species [Figs. 4(b) and 4(c)], we find no effect in the preedge region although the effects on the main- and postedge regions are in closer agreement with observation than symmetric expansion [Fig. 4(a)]. This suggests that the main difference between the isotopes is that asymmetric SD species in H_2O on average are more asymmetric than corresponding species in D_2O. Although not contributing to the observed differences in the preedge region, we cannot exclude minor contributions from asymmetric distortions of symmetrically H-bonded DD species in the higher spectral energy range. Apart from the qualitative agreement, we observe that the intensity difference is considerably larger in the theoretical simulations [Figs. 1(a)–1(c)]. A more rigorous analysis including averaging over many structural motifs and distortions would decrease the intensity differences relative to the single "average cases" considered here. Nevertheless, the comparison between experiment and theory suggests (if anything) that the absolute geometrical change in asymmetry, on average, is smaller than the case considered in, e.g., Fig. 4(c) (0.2 Å elongation and 0.05 Å shortening).

Finally, the comparison also shows that a temperature effect of 20 °C [Fig. 4(e)] does not fit as well to these model calculations. A better agreement is found for the isotope difference at RT [Fig. 3(c)] and the isotope difference with a 10 °C temperature effect subtracted [Fig. 4(d)], consistent with the reported temperature offset of ~5 °C as derived from γ- and x-ray-diffraction data.[16,36] Furthermore, a simple thermodynamical shift model based on experimental isochoric temperature and isothermal density differential functions fails to describe the magnitude of the isotopic differences seen in x-ray-diffraction data at temperatures below 310 K, where much larger changes are observed.[36] The isotope effects investigated here with XRS might provide an explanation of this observation in terms mainly of a larger local asymmetry of SD species in H_2O as needed to correctly describe the differences between H_2O and D_2O.

We conclude that the difference between liquid H_2O and D_2O is discernible in XA as probed by XRS. By comparing the difference spectrum between room-temperature H_2O and D_2O to the temperature difference spectrum of H_2O at 22 and 2 °C, we find that the spectral changes in D_2O can partly be understood by an effect similar to a lowering of the temperature, as has also been reported in diffraction studies.[16,36] In addition, a small but significant dissimilarity between the isotope and temperature difference spectra is noticeable. We attribute this dissimilarity to an increase in local H-bond asymmetry on the donor sides for H_2O relative to D_2O. This previously unreported asymmetry effect indicates the high sensitivity of XA to the local structure. Based on our results, we suggest that quantum effects, as evidenced through the influence of the different masses on the XA spectrum, play a role in the formation of asymmetrical (SD) species in liquid water.

This work was supported by the National Science Foundation under Grants No. CHE-0431425 and No. CHE-0518637, the Swedish Foundation for Strategic Research, and the Swedish Natural Science Research Council. D.N. conducted the work under a postdoctoral grant from the Wenner-Gren Foundations. Portions of this research were carried out at the Stanford Synchrotron Radiation Laboratory, a national user facility operated by Stanford University on behalf of the U.S. Department of Energy, Office of Basic Energy Sciences. Use of the Advanced Photon Source was supported by the U.S. Department of Energy, Basic Energy Sciences, Office of Science, under Contract No. W-31-109-ENG-38. BioCAT is a National Institutes of Health-supported Research Center RR-08630. Assistance by the APS beamline 18-ID staff is gratefully acknowledged.

[1] Ph. Wernet, D. Nordlund, U. Bergmann, M. Cavalleri, M. Odelius, H. Ogasawara, L. A. Näslund, T. K. Hirsch, L. Ojamäe, P. Glatzel, L. G. M. Pettersson, and A. Nilsson, Science **304**, 995 (2004).

[2] A. K. Soper, J. Phys.: Condens. Matter **17**, S3273 (2005).

[3] T. Head-Gordon and M. Johnson, Proc. Natl. Acad. Sci. U.S.A. **103**, 7973 (2006); **103**, 16614(E) (2006); M. Leetmaa, M. Ljungberg, H. Ogasawara, M. Odelius, L. A. Näslund, A. Nilsson, and L. G. M. Pettersson, J. Chem. Phys. **125**, 244510 (2006).

[4] G. Hura, D. Russo, R. M. Glaeser, T. Head-Gordon, M. Krack, and M. Parrinello, Phys. Chem. Chem. Phys. **5**, 1981 (2003).

[5] A. K. Soper, Mol. Phys. **99**, 1503 (2001); Chem. Phys. **202**, 295 (1996).

[6] A. K. Soper (private communication); J. D. Smith, C. D. Cappa, B. M. Messer, W. S. Drisdell, R. C. Cohen, and R. J. Saykally,

J. Phys. Chem. B **110**, 20038 (2006); T. Head-Gordon and S. W. Rick, Phys. Chem. Chem. Phys. **9**, 83 (2007).

[7] Y. A. Mantz, B. Chen, and G. J. Martyna, Chem. Phys. Lett. **405**, 294 (2005); J. Phys. Chem. B **110**, 3540 (2006); D. Prendergast and G. Galli, Phys. Rev. Lett. **96**, 215502 (2006); D. Prendergast, J. C. Grossman, and G. Galli, J. Chem. Phys. **123**, 014501 (2005); J. D. Smith, C. D. Cappa, B. M. Messer, R. C. Cohen, and R. J. Saykally, Science **308**, 793b (2005); J. D. Smith, C. D. Cappa, K. R. Wilson, B. M. Messer, R. C. Cohen, and R. J. Saykally, *ibid.* **306**, 851 (2004); M. Cavalleri, M. Odelius, D. Nordlund, A. Nilsson, and L. G. M. Pettersson, Phys. Chem. Chem. Phys. **7**, 2854 (2005).

[8] A. Nilsson, Ph. Wernet, D. Nordlund, U. Bergmann, M. Cavalleri, M. Odelius, H. Ogasawara, L. A. Näslund, T. K. Hirsch, P. Glatzel, and L. G. M. Pettersson, Science **308**, 793a (2005).

[9] F. Weinhold, Adv. Protein Chem. **72**, 121 (2006).

[10] M. Odelius, M. Cavalleri, A. Nilsson, and L. G. M. Pettersson, Phys. Rev. B **73**, 024205 (2006).

[11] L. Å. Näslund, J. Lüning, Y. Ufuktepe, H. Ogasawara, Ph. Wernet, U. Bergmann, L. G. M. Pettersson, and A. Nilsson, J. Phys. Chem. B **109**, 13835 (2005).

[12] G. Némethy and H. A. Scheraga, J. Chem. Phys. **41**, 680 (1964).

[13] P. A. Egelstaff, Phys. Chem. Liq. **40**, 203 (2002).

[14] J. H. Root, P. A. Egelstaff, and A. Hime, Chem. Phys. **109**, 437 (1986).

[15] C. H. Cho, J. Urquidi, S. Singh, and G. W. Robinson, J. Phys. Chem. B **103**, 1991 (1999); M. Vedamuthu, S. Singh, and G. W. Robinson, J. Phys. Chem. **98**, 8591 (1994).

[16] B. Tomberli, C. J. Benmore, P. A. Egelstaff, J. Neuefeind, and V. Honkimaki, J. Phys.: Condens. Matter **12**, 2597 (2000); Y. S. Badyal, D. L. Price, M. L. Saboungi, D. R. Haeffner, and S. D. Shastri, J. Chem. Phys. **116**, 10833 (2002); R. T. Hart, C. J. Benmore, J. Neuefeind, S. Kohara, B. Tomberli, and P. A. Egelstaff, Phys. Rev. Lett. **94**, 047801 (2005).

[17] R. A. Kuharski and P. J. Rossky, Chem. Phys. Lett. **103**, 357 (1984); J. Chem. Phys. **82**, 5289 (1985); A. Wallqvist and B. J. Berne, Chem. Phys. Lett. **117**, 214 (1985); G. S. Delbuono, P. J. Rossky, and J. Schnitker, J. Chem. Phys. **95**, 3728 (1991); S. R. Billeter, P. M. King, and W. F. Vangunsteren, *ibid.* **100**, 6692 (1994); B. Guillot and Y. Guissani, Fluid Phase Equilib. **151**, 19 (1998); J. Lobaugh and G. A. Voth, J. Chem. Phys. **106**, 2400 (1997); B. Chen, I. Ivanov, M. L. Klein, and M. Parrinello, Phys. Rev. Lett. **91**, 215503 (2003).

[18] L. Hernández de la Peña and P. G. Kusalik, J. Am. Chem. Soc. **127**, 5246 (2005).

[19] M. G. Brown, F. N. Keutsch, and R. J. Saykally, J. Chem. Phys. **109**, 9645 (1998).

[20] F. N. Keutsch, J. D. Cruzan, and R. J. Saykally, Chem. Rev. (Washington, D.C.) **103**, 2533 (2003).

[21] F. Weinhold, J. Mol. Struct.: THEOCHEM **398**, 181 (1997).

[22] R. Ludwig and F. Weinhold, Z. Phys. Chem. **216**, 659 (2002).

[23] U. Bergmann, P. Glatzel, and S. P. Cramer, Microchem. J. **71**, 221 (2002); M. Krisch and F. Sette, Surf. Rev. Lett. **9**, 969 (2002); Y. Q. Cai, H.-K. Mao, P. C. Chow, J. S. Tse, Y. Ma, S. Patchkovskii, J. F. Shu, V. Struzhkin, R. J. Hemley, H. Ishii, C. C. Chen, I. Jarrige, C. T. Chen, S. R. Shieh, E. P. Huang, and C. C. Kao, Phys. Rev. Lett. **94**, 025502 (2005).

[24] U. Bergmann, Ph. Wernet, P. Glatzel, M. Cavalleri, L. G. M. Pettersson, A. Nilsson, and S. P. Cramer, Phys. Rev. B **66**, 092107 (2002).

[25] D. T. Bowron, M. H. Krisch, A. C. Barnes, J. L. Finney, A. Kaprolat, and M. Lorenzen, Phys. Rev. B **62**, R9223 (2000).

[26] J. Stöhr, *NEXAFS Spectroscopy* (Springer-Verlag, Berlin, 1992).

[27] We also found that if the water is in a small isolated sample space (<1 ml), gas bubbles resulting from hydrolyzation can be trapped at the location where the beam interacts with the sample, which in turn can decrease the intensity of the scattering signal.

[28] The spectra shown in all figures (including theoretical spectra) are normalized by setting the intensity integral over 532–550 eV equal to 1000. As a result, the maximum (main edge) intensity is close to 100 and the absolute intensity for the difference spectra shown in the figures can approximately be translated to percent of maximum intensity.

[29] M. Cavalleri, H. Ogasawara, L. G. M. Pettersson, and A. Nilsson, Chem. Phys. Lett. **364**, 363 (2002).

[30] J. Schirmer, A. B. Trofimov, K. J. Randall, J. Feldhaus, A. M. Bradshaw, Y. Ma, C. T. Chen, and F. Sette, Phys. Rev. A **47**, 1136 (1993).

[31] M. Cavalleri, L. A. Näslund, D. C. Edwards, Ph. Wernet, H. Ogasawara, S. Myneni, L. Ojamäe, M. Odelius, A. Nilsson, and L. G. M. Pettersson, J. Chem. Phys. **124**, 194508 (2006).

[32] W. F. Kuhs and M. S. Lehmann, Water Sci. Rev. **2**, 1 (1986).

[33] R. Ludwig, Angew. Chem., Int. Ed. **40**, 1809 (2001); S. S. Xantheas, Chem. Phys. **258**, 225 (2000).

[34] K. Hermann, L. G. M. Pettersson, M. E. Casida, C. Daul, A. Goursot, A. Koester, E. Proynov, A. St-Amant, D. R. Salahub, V. Carravetta, A. Duarte, N. Godbout, J. Guan, C. Jamorski, M. Leboeuf, V. Malkin, O. Malkina, M. Nyberg, L. Pedocchi, F. Sim, L. Triguero, and A. Vela, STOBE, Stockholm-Berlin-Montreal, 2005.

[35] K. R. Wilson, M. Cavalleri, B. S. Rude, R. D. Schaller, T. Catalano, A. Nilsson, R. J. Saykally, and L. G. M. Pettersson, J. Phys. Chem. B **109**, 10194 (2005).

[36] R. T. Hart, Q. Mei, C. J. Benmore, J. C. Neuefeind, J. F. C. Turner, M. Dolgos, B. Tomberli, and P. A. Egelstaff, J. Chem. Phys. **124**, 134505 (2006).